J. Phys. Chem. A **2000,** *104,* 11297−11303

Calculated CH-Stretching Overtone Spectra of Naphthalene, Anthracene and Their Cations

Henrik G. Kjaergaard,* Timothy W. Robinson, and Karleen A. Brooking

Department of Chemistry, University of Otago, P.O. Box 56, Dunedin, New Zealand

Received: July 27, 2000

We have calculated fundamental and overtone CH-stretching vibrational band frequencies and intensities of neutral and cationic naphthalene and anthracene, the smallest of the polycyclic aromatic hydrocarbons. The calculations use a simple anharmonic oscillator local mode model with local mode parameters obtained from scaled ab initio calculations and ab initio calculated dipole moment functions. The ab initio calculations were performed at the self-consistent-field Hartree−Fock and the B3LYP hybrid density functional levels of theory with the 6-31G(d) and 6-311+G(d,p) basis sets. The vapor phase overtone spectra of anthracene and both cations have not yet been observed. We find that the cation frequencies are blue shifted and the overtone transitions are of comparable intensities to those in the neutral molecules, contrary to the fundamental transitions which are significantly weaker in the cations. The method presented here can provide an accurate estimate of CH-stretching overtone spectra of neutral and cationic polycyclic aromatic hydrocarbons.

Introduction

Near-infrared (NIR) spectra are dominated by XH-stretching overtone vibrations, where X is a heavy atom such as C, O, or N. The large amplitude motion associated with XH-stretching vibrations has been explained well by the harmonically coupled anharmonic oscillator (HCAO) local mode model.[1−5] More recently, overtone intensities have been successfully predicted with use of vibrational wave functions obtained with the HCAO local mode model and ab initio calculated dipole moment functions.[6−13]

We have investigated the effects of basis set size and choice of theory on vibrational band intensities for H_2O and other small molecules.[14−16] Comparison of the HCAO method with a full variational calculation indicated that the simple HCAO method was adequate.[17] Basis sets in the range 6-31G(d) to 6-311++G(3df,3pd), and theoretical methods including uncorrelated and correlated ab initio, and density functional theories have been tested.[14−16] It was found that electron correlation is more important for fundamental intensities than for overtones, and less surprisingly, that the calculated intensities converge with increasing basis set size. The apparent insensitivity to electron correlation of the calculated overtone intensities has been observed for OH-, CH- and NH-stretching oscillators in a range of molecules. We have found that relative intensities within an overtone are predicted correctly with an ab initio dipole moment function calculated with the self-consistent-field Hartree−Fock theory and a 6-31G(d) basis set (HF/6-31G(d)) and have suggested that spectroscopically useful absolute intensities could be calculated with an HF/6-311+G(d,p) dipole moment function.[13−16]

We have recently suggested a method that will allow the calculation of overtone spectra of molecules for which no overtone spectra have been recorded. We have applied this method to the water dimer[18] which has subsequently allowed an assessment of the importance of the water dimer as an absorber of solar radiation.[19] The calculated overtone spectrum of the water dimer was in qualitative agreement with recent laboratory and atmospheric investigations.[20,21]

There is strong evidence for the presence of polycyclic aromatic hydrocarbons (PAHs) in the interstellar medium.[22−24] Spectroscopic transitions (electronic and vibrational) in PAHs and/or their derivatives are suspected to be contributors to the unidentified infrared (UIR) bands and the diffuse interstellar bands (DIB).[25−28] There have been a number of experimental and theoretical studies of neutral and cationic PAHs.[25−38] These studies have focused primarily on the fundamental infrared (IR) region with few studies of the overtone spectra of PAHs and/or their derivatives.

We have previously measured the vapor and solid-phase CH-stretching overtone spectra of naphthalene, the smallest of the PAHs.[33,34] In the present paper, we investigate calculated fundamental and overtone CH-stretching spectra of naphthalene and anthracene, and their cations. We have calculated the CH-stretching vibrational band frequencies and intensities with the use of a simple anharmonic oscillator (AO) local mode model with local mode parameters obtained from scaled ab initio calculations and ab initio calculated dipole moment functions. The ab initio calculations were performed with the HF and B3LYP hybrid density functional theories and the 6-31G(d) and 6-311+G(d,p) basis sets, which we label basis sets I and II, respectively. Vapor phase overtone spectra of anthracene and both cations have not yet been observed. The most recent fundamental IR spectra of these PAHs are from matrix isolation studies.[30,31]

The unpaired electron in cations poses a challenge to the ab initio calculations. Bauschlicher and Langhoff recently showed that the HF theory was not suitable for the calculation of IR intensities of the naphthalene cation.[36] However, they showed that the B3LYP theory provided reasonable IR frequencies and intensities. Langhoff has calculated IR frequencies and intensities for a series of neutral and cationic PAHs which showed quite good agreement with the available experimental data.[35] These calculations have all used the so-called double harmonic

---

* Corresponding author. E-mail: henrik@alkali.otago.ac.nz. Fax: +64-3-479-7906.

10.1021/jp002686n CCC: $19.00

(DH) approximation, which uses a linear dipole moment function and a harmonic oscillator for each of the normal modes. In general, these DH calculations of PAH cations show a small blue shift of the fundamental CH-stretching frequencies and a significant drop in the fundamental CH-stretching intensity compared to the neutral molecule. We have compared our AO calculated results to those calculated with the DH approximation.

For the CH-stretching overtones our calculations show that the cation frequencies are blue shifted and the transitions are of comparable intensity to those of the neutral molecules, although changes in the relative intensities within an overtone are observed between the neutral and cationic species. We suggests that the method presented in this paper can provide accurate simulations of CH-stretching overtone spectra of neutral and cationic PAHs. These simulated NIR spectra could assist in the identification of interstellar spectra.

Theory and Calculations

The oscillator strength f of a transition from the ground vibrational state g to an excited state e is given by[10,39]

$$f_{\mathrm{eg}} = 4.702 \times 10^{-7}\,[\mathrm{cm\ D^{-2}}]\ \tilde{\nu}_{\mathrm{eg}}|\vec{\mu}_{\mathrm{eg}}|^2 \tag{1}$$

where $\tilde{\nu}_{\mathrm{eg}}$ is the vibrational wavenumber of the transition in cm^{-1} and $\vec{\mu}_{\mathrm{eg}} = \langle \mathrm{e}|\vec{\mu}|\mathrm{g}\rangle$ is the transition dipole moment matrix element in Debye (D). Thus, to calculate vibrational band intensities and simulate overtone spectra we need to obtain both the vibrational wave functions and the dipole moment function. Experimental vibrational intensities are commonly given as absorption coefficients with units km mol^{-1} for fundamental transitions and integrated cross sections with units cm molecule^{-1} for overtones. Conversions of the dimensionless oscillator strength to km mol^{-1} and cm molecule^{-1} are: 5.33×10^6 km mol^{-1} × f and 8.85×10^{-13} cm molecule^{-1} × f, respectively.

Vibrational Model. The CH bonds in PAHs can, to a good approximation, be treated as isolated anharmonic CH-stretching local modes with no coupling between them and no coupling to other vibrational modes.[11,13,33] The isolated local modes are described by Morse oscillators with one set of local mode parameters for each of the nonequivalent CH oscillators in the molecules. The Hamiltonian of a Morse oscillator can be written

$$(H - E_{|0\rangle j})/hc = v_j\tilde{\omega}_j - (v_j^{\,2} + v_j)\tilde{\omega}x_j \tag{2}$$

where $E_{|0\rangle j}$ is the energy of the vibrational ground state and $\tilde{\omega}_j$ and $\tilde{\omega}x_j$ are the local mode frequency and anharmonicity (in cm^{-1}) of the CH$_j$ oscillator. The eigenstates of the Hamiltonian are denoted by $|v_j\rangle_j$ where v_j is the vibrational quantum number. These eigenstates are thus Morse oscillator wave functions. The local mode parameters $\tilde{\omega}$ and $\tilde{\omega}x$ are usually derived from a fit of the observed local mode peak positions $\bar{\nu}$ to a two-parameter Morse oscillator expression[33]

$$\bar{\nu}/v = \tilde{\omega} - (v + 1)\tilde{\omega}x \tag{3}$$

This is obviously only possible for molecules for which the overtone transitions have been observed. We have previously used this method to determine the local mode parameters for naphthalene from the observed vapor phase overtone spectra.[33] We have used a method based on ab initio calculated potential energy curves to obtain the local mode parameters for anthracene and both cations.

Ab Initio Determination of Local Mode Parameters. The Morse oscillator frequency $\tilde{\omega}$ and anharmonicity $\tilde{\omega}x$ can be expressed by the second and third order ab initio calculated force constants F_{ii} and F_{iii} by[18,40]

$$\tilde{\omega} = \frac{\omega}{2\pi c} = \frac{(F_{ii}G_{ii})^{1/2}}{2\pi c} \tag{4}$$

$$\tilde{\omega}x = \frac{\omega x}{2\pi c} = \frac{hG_{ii}}{72\pi^2 c}\left(\frac{F_{iii}}{F_{ii}}\right)^2 \tag{5}$$

where the Wilson **G** matrix element $G_{ii} = 1/\mu$ and μ is the reduced mass of the CH oscillator. The force constants are the derivatives of the potential energy $V(q)$ with respect to the internal displacement coordinate, q. We calculate the force constants by standard numerical techniques from a one-dimensional grid of ab initio calculated potential energies $V(q)$.[41] The grid is calculated by displacing the internal coordinate from the equilibrium position. These one-dimensional grids are also used to obtain the dipole moment function (vide infra).

We have scaled our ab initio calculated local mode parameters similarly to the common practice of scaling ab initio calculated IR frequencies. It is important to note that the scaling of IR frequencies is done both to compensate for deficiencies in the ab initio method and the inherent anharmonicity of the vibrational modes. However, the scaling of the local mode parameters is done only to compensate for the deficiencies in the ab initio method. We have used the accurate experimental local mode parameters for the CH$_\alpha$ and CH$_\beta$ oscillators from vapor phase naphthalene overtone spectra to determine scaling factors which we believe are suitable for CH-stretching oscillators in neutral and cationic PAHs. We have taken the scaling factors as the average between the scaling found for the CH$_\alpha$ and CH$_\beta$ oscillators in neutral naphthalene. The experimental local mode parameters were determined by fitting the observed CH-stretching transitions in the $\Delta v_{\mathrm{CH}} = 2-6$ regions to eq 3 and led to standard deviations of ±2 cm^{-1} and ±0.3 cm^{-1} for $\tilde{\omega}$ and $\tilde{\omega}x$, respectively.[34]

Dipole Moment Function. For an isolated CH oscillator, we express the dipole moment function as a series expansion in the displacement coordinate,[11,13]

$$\vec{\mu}(q) = \sum_i \vec{\mu}_i q^i \tag{6}$$

where $\vec{\mu}_i$ is $1/i!$ times the ith order derivative of the dipole moment function with respect to q. The coefficients $\vec{\mu}_i$ are calculated by standard numerical techniques from the one-dimensional dipole moment grid, $\vec{\mu}(q)$.[10,41] The grid is calculated by displacing the internal displacement coordinate by ±0.2 Å from the equilibrium position in steps of 0.05 Å. This series of single point ab initio calculations provides both $V(q)$ and $\vec{\mu}(q)$. The choice of grid and step size is based on previous work.[18] The nine point grid with a step size of 0.05 Å was found to provide a good convergence of the dipole moment derivatives to sixth order and force constants to third order.

The optimized geometries and all points in a grid were calculated at a specified ab initio method with the use of Gaussian94.[42] Values of the dipole moment were calculated with use of the generalized density for the specified level of theory (density = current) to provide dipole moments that are the correct analytical derivatives of the energy. The convergence of the dipole derivatives was poorer than expected for the cations. We increased the numerical integration grid size used in the B3LYP module within Gaussian94 from the default FineGrid (a pruned version of the 77302 grid) to a larger grid

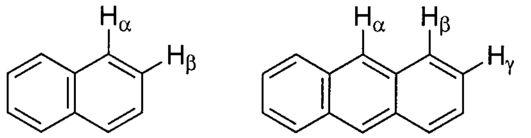

Figure 1. B3LYP/II optimized structures and labeling of naphthalene and anthracene. The calculated CH bond lengths are $CH_\alpha = 1.085$ Å (1.084) and $CH_\beta = 1.084$ Å (1.083) for naphthalene, and $CH_\alpha = 1.086$ Å (1.085), $CH_\beta = 1.085$ Å (1.084) and $CH_\gamma = 1.084$ Å (1.083) for anthracene, with the cation bond lengths given in brackets.

TABLE 1: Local Mode Frequency and Anharmonicity Scaling Factors[a]

	sf_ω	$sf_{\omega x}$
HF/I	0.9386	0.905
B3LYP/I	0.9903	0.857
B3LYP/II	0.9965	0.884

[a] Calculated with use of the experimental local mode parameters for naphthalene from ref 34.

(Grid = 99434) to improve convergence of the expansion coefficients. The convergence of the sixth order expansion coefficients was still not satisfactory for the cations and thus we have limited the expansion in eq 6 to fifth order. An increase in integration grid size has a significant effect on the required computer time. Calculations with the 99434 grid are about four times more expensive than calculations with the default grid.

We have previously investigated the effects of basis set size and choice of ab initio theory in the dipole moment function on the calculated vibrational band intensities.[14−16] We found that nonlocal and hybrid DFT methods provided intensities of similar quality to QCISD methods. On the basis of these previous investigations we have limited the present study to the HF and B3LYP theories with the basis sets I and II.

Results and Discussion

The B3LYP/II optimized structures and labeling used for naphthalene and anthracene are shown in Figure 1. We have optimized the structures using the "tight" convergence criterion within Gaussian94. Our optimized geometry of the naphthalene cation is in good agreement with similar previous calculations.[32,36] The B3LYP calculations correctly predict D_{2h} symmetry for naphthalene, anthracene and their cations. The B3LYP/II optimized CH bond lengths are given in the caption to Figure 1. The CH bond lengths decrease with increasing distance from the center of the molecule. The decrease is approximately 1 mÅ from CH_α to CH_β (and to CH_γ). Ionization systematically shortens the CH bond lengths by about 1 mÅ.

In agreement with Bauschlicher and Langhoff[36] we find that HF calculations of the naphthalene cation yield a lower symmetry C_{2h} geometry, where the two CH_α bonds in the same ring differ by less than 1 mÅ and similarly for the CH_β bonds. The problem results from the HF theory's inability to properly delocalize the positive charge. We also optimized the naphthalene cation restrained to D_{2h} symmetry with the HF method. The D_{2h} structure has a slightly higher energy (0.31 mHartree) and one imaginary frequency. However, the D_{2h} solution has less spin contamination of the wave function. The HF method correctly predicts the D_{2h} structure for the neutral molecules.

Scaling Factors and Local Mode Parameters. We have scaled the ab initio calculated local mode frequencies and anharmonicities in a similar way to the scaling of DH calculated frequencies. The scaling factors obtained for each of the *ab initio* methods are given in Table 1. The scaling factors are all less than unity. The scaling required for the frequencies is less than that required for the anharmonicities. The scaling factor for the B3LYP/II frequencies is particularly close to unity.

TABLE 2: Scaled Local Mode Parameters (cm^{-1}) for Naphthalene Cation[a]

	naphthalene cation				naphthalene
	HF/I[b]	HF/I[c]	B3LYP/I	B3LYP/II	exp[d]
$\tilde{\omega}_\alpha$	3186	3187	3184	3177	3153
$\tilde{\omega}_{\alpha'}$		3187			
$\tilde{\omega}_\beta$	3198	3196	3200	3191	3170
$\tilde{\omega}_{\beta'}$		3201			
$\tilde{\omega}x_\alpha$	57.7	57.7	57.6	57.6	58.3
$\tilde{\omega}x_{\alpha'}$		57.8			
$\tilde{\omega}x_\beta$	57.5	57.5	57.3	57.4	58.7
$\tilde{\omega}x_{\beta'}$		57.5			

[a] Calculated ab initio and scaled with scaling factors from Table 1. The α and α′ refer to the two nonequivalent CH_α oscillators for the C_{2h} structure, and similarly for CH_β. [b] D_{2h} structure. [c] C_{2h} structure. [d] From ref 34.

TABLE 3: Scaled Local Mode Parameters (cm^{-1}) for Anthracene and Anthracene Cation[a]

	anthracene			anthracene cation	
	HF/I	B3LYP/I	B3LYP/II	B3LYP/I	B3LYP/II
$\tilde{\omega}_\alpha$	3151	3147	3149	3171	3167
$\tilde{\omega}_\beta$	3158	3157	3157	3182	3177
$\tilde{\omega}_\gamma$	3166	3168	3167	3196	3188
$\tilde{\omega}x_\alpha$	58.6	58.7	58.7	57.9	57.8
$\tilde{\omega}x_\beta$	58.6	58.6	58.6	57.7	57.7
$\tilde{\omega}x_\gamma$	58.5	58.4	58.4	57.5	57.5

[a] Calculated ab initio and scaled with the scaling factors from Table 1.

The scaled local mode parameters for the naphthalene cation and the experimentally determined values from the vapor phase spectra of neutral naphthalene are given in Table 2. The scaled parameters for the cation are similar for the various methods used and we estimate the errors in $\tilde{\omega}$ and $\tilde{\omega}x_j$ to be less than 10 and 1 cm^{-1}, respectively. This degree of uncertainty in the local mode parameters is in agreement with previous studies and gives rise to very small differences in the calculated intensities.[18]

The HF/I calculated local mode parameters for the C_{2h} and D_{2h} structures of naphthalene are similar as might be expected from the similar structures. In the lower energy C_{2h} structure small differences are seen between the two nonequivalent CH_α oscillators.

The scaled local mode parameters for anthracene and the anthracene cation are given in Table 3. The variation in the scaled frequencies and anharmonicities is very small for anthracene and slightly larger for the anthracene cation. From Tables 2 and 3 we see that the CH-oscillators in cations have higher frequencies and slightly smaller anharmonicities compared to the neutral molecules. The higher frequencies in the cations are in agreement with the corresponding calculated bond lengths and we would expect CH-stretching transitions in the cations to be blue shifted. The difference in anharmonicities between the neutral and cationic species is very small and is not expected to lead to any significant intensity changes. Thus, any difference in intensity between the two species must arise from changes in the dipole moment function.

Fundamental Transitions. The fundamental spectrum of naphthalene and its cation will have eight vibrational transitions where the associated normal modes are predominantly CH-stretching motion. The four ungerade vibrations, two each of b_{1u} and b_{2u} symmetry, are IR allowed. Coupling between CH_α and CH_β oscillators causes the normal modes to contain both

TABLE 4: Fundamental CH-Stretching Total Oscillator Strengths for Neutral and Cationic Naphthalene and Anthracene[a]

	naphthalene		anthracene	
	neutral	cation	neutral	cation
DH[b]	3.00×10^{-5}		3.87×10^{-5}	1.58×10^{-6}
DH/I	2.60×10^{-5}	2.28×10^{-7}	3.34×10^{-5}	1.33×10^{-6}
DH/II	1.92×10^{-5}	6.76×10^{-7}	2.48×10^{-5}	3.50×10^{-7}
AO/I[c]	3.08×10^{-5}	6.73×10^{-7}	3.93×10^{-5}	3.23×10^{-7}
AO/II[c]	2.41×10^{-5}	1.63×10^{-6}	3.10×10^{-5}	9.08×10^{-8}
exp[d]	1.0×10^{-6}			
exp[e]	8.9×10^{-6}		2.1×10^{-5}	

[a] All calculations at the B3LYP level of theory. [b] B3LYP/4-31G calculation from ref 35. [c] Calculated with the local mode parameters from Tables 2 and 3. [d] From ref 31. [e] From ref 30.

CH_α- and CH_β-stretching character. In our AO local mode calculations the small coupling between CH oscillators is neglected, resulting in only two transitions in the fundamental region and each of the overtone regions. Thus, a comparison of individual CH-stretching transitions obtained with the DH and AO approximations is not meaningful. However, a comparison of the total fundamental CH-stretching intensity will illustrate the importance that anharmonicity in the potential and deviations from linearity in the dipole moment function have on the fundamental CH-stretching intensities. Similarly, for anthracene there are ten predominantly CH-stretching normal modes and only three nonequivalent local modes.

Calculated and experimental total fundamental CH-stretching intensities are compared in Table 4. Both the AO and DH methods predict more than an order of magnitude decrease in total CH-stretching intensity for the cations compared to the neutral species. The significant drop in intensity for the ionized species agrees with previous theoretical studies and with matrix isolation experimental studies, which have so far failed to observed CH-stretching bands in the spectra of naphthalene and anthracene cations.[30,31] The difference between total CH-stretching intensities calculated with the DH and AO methods is about 20% for the neutral species and a factor of two to four for the cationic species. This difference arises mainly from the approximations in the DH method. The significant decrease in intensity of the total fundamental CH-stretching intensity upon ionization is primarily due to changes in the dipole moment function since the calculated anharmonicities of the CH oscillators are very similar for the neutral and cationic species. Inspection of the dipole moment function for neutral naphthalene shows that the second-order term in the dipole moment function expansion contributes about 25% to the intensity, in agreement with the difference seen between the intensities calculated with the AO and DH methods. The first and second coefficients $\vec{\mu}_1$ and $\vec{\mu}_2$ have the same sign and since the integrals $\langle 1|q|0\rangle$ and $\langle 1|q^2|0\rangle$ also have the same sign the intensity contributions are additive. The dipole moment function is very different for the naphthalene cation. The $\vec{\mu}_1$ coefficient is much smaller leading to a significantly lower fundamental intensity with a more significant contribution from the second-order term. Furthermore, the signs of $\vec{\mu}_1$ and $\vec{\mu}_2$ are opposite and the intensity contributions from these two terms to some extent cancel. This explains the significant decrease in fundamental intensity for the cations and also the large discrepancy between intensities calculated with the AO and DH methods.

For the neutral molecules both the AO and DH calculated fundamental intensities decrease by about 25% with increasing the basis set size from I to II, as expected.[14,36] The intensity increases by a factor of about three from basis set I to II for the naphthalene cation whereas it decreases by a factor of about three for the anthracene cation as seen in Table 4.

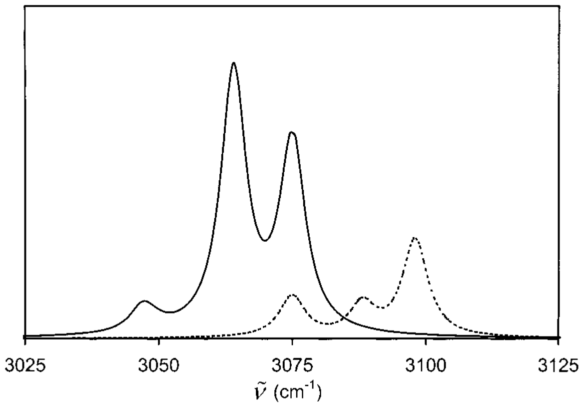

Figure 2. Simulated spectra of naphthalene (solid line) and naphthalene cation (dotted line) in the fundamental region ($\Delta v_{CH} = 1$). The vibrational transitions have been calculated with the B3LYP/II method and DH approximation. The vibrational frequencies have been scaled by 0.965 and the cation intensities multiplied by a factor of 10. Each transition has been convoluted with a Lorentzian with a full width at half-maximum of 6 cm^{-1}.

The calculated total fundamental CH-stretching intensities are larger than the experimental values for neutral naphthalene and neutral anthracene. In both cases the calculated intensities are within a factor of three of the experimental values. No experimental CH-stretching fundamental spectra for the cations are available.

Simulated IR spectra of naphthalene and naphthalene cation are shown in Figure 2. The spectra have been generated from DH IR frequencies and intensities calculated with the B3LYP/II method. The frequencies have been scaled by a factor of 0.965 determined from the ratio of experimental to calculated frequencies of the two strong (b_{1u} and b_{2u}) CH-stretching normal modes in naphthalene.[30] Each transition has been convoluted with a Lorentzian with a full width at half-maximum (fwhm) of 6 cm^{-1}. The cation spectrum has been multiplied by a factor of ten to facilitate comparison. The figure shows a blue shift of about 25 cm^{-1}, a change in spectral profile, and a significant drop in intensity on ionization.

Overtone Transitions. The problem encountered with HF optimization of the naphthalene cation suggests that HF theory, which has been found to calculate overtone intensities in neutral molecules very well, might not be suitable for cations. Problems were encountered with convergence of the HF energy and the dipole moment derivatives. The higher order terms in the expansion of the dipole moment function were very large.

We have tested the effect that the numerical integration grid size used in the DFT module within Gaussian94 has on the calculated intensities. In Table 5 we show calculated intensities of the transitions to the $|v\rangle_\alpha$ and $|v\rangle_\beta$ states in naphthalene with different numerical integration grids sizes ranging from the default FineGrid to the 99590 grid. The 99590 grid has $99 \times 590 = 58410$ points while FineGrid has about 7000 points.[42] The optimized geometry and each point in the dipole moment grid were calculated with the specified numerical integration grid size. We see in Table 5 that the fundamental and lower overtone intensities are well converged with the default integration grid. For the higher overtones some variation in the intensities is apparent with changing integration grid size. The variation seems to be less than 20% for the range of grids tested. We have chosen to use the 99434 grid in our B3LYP calculations of overtone intensities. Comparison with a few somewhat larger integration grids suggests that the uncertainty

TABLE 5: Calculated Oscillator Strengths of the CH-Stretching Transitions in Naphthalene at the B3LYP/I Level with Different Numerical Integration Grid Sizes[a]

	Grid					
	FineGrid[b]	75302	75434	99434	125434	99590
$\|1\rangle_\alpha$	1.31×10^{-5}	1.31×10^{-5}	1.31×10^{-5}	1.31×10^{-5}	1.31×10^{-5}	1.31×10^{-5}
$\|1\rangle_\beta$	1.77×10^{-5}	1.77×10^{-5}	1.77×10^{-5}	1.77×10^{-5}	1.77×10^{-5}	1.77×10^{-5}
$\|2\rangle_\alpha$	3.75×10^{-7}	3.76×10^{-7}	3.73×10^{-7}	3.73×10^{-7}	3.73×10^{-7}	3.73×10^{-7}
$\|2\rangle_\beta$	5.72×10^{-7}	5.53×10^{-7}	5.53×10^{-7}	5.50×10^{-7}	5.50×10^{-7}	5.71×10^{-7}
$\|3\rangle_\alpha$	6.99×10^{-8}	6.98×10^{-8}	7.02×10^{-8}	6.97×10^{-8}	6.97×10^{-8}	6.95×10^{-8}
$\|3\rangle_\beta$	1.08×10^{-7}	1.15×10^{-7}	1.14×10^{-7}	1.14×10^{-7}	1.14×10^{-7}	1.07×10^{-7}
$\|4\rangle_\alpha$	7.45×10^{-9}	7.47×10^{-9}	7.31×10^{-9}	7.34×10^{-9}	7.33×10^{-9}	7.35×10^{-9}
$\|4\rangle_\beta$	1.25×10^{-8}	1.12×10^{-8}	1.13×10^{-8}	1.11×10^{-8}	1.11×10^{-8}	1.25×10^{-8}
$\|5\rangle_\alpha$	9.75×10^{-10}	9.71×10^{-10}	8.99×10^{-10}	8.75×10^{-10}	8.68×10^{-10}	8.62×10^{-10}
$\|5\rangle_\beta$	1.69×10^{-9}	1.48×10^{-9}	1.42×10^{-9}	1.35×10^{-9}	1.35×10^{-9}	1.57×10^{-9}
$\|6\rangle_\alpha$	1.56×10^{-10}	1.53×10^{-10}	1.34×10^{-10}	1.24×10^{-10}	1.22×10^{-10}	1.19×10^{-10}
$\|6\rangle_\beta$	2.72×10^{-10}	2.55×10^{-10}	2.29×10^{-10}	2.08×10^{-10}	2.08×10^{-10}	2.25×10^{-10}

[a] Grid is the size of the grid that is used for numerical integration within Gaussian94. [b] FineGrid is the default in Gaussian94 and is a pruned version of the 75302 grid.

TABLE 6: Calculated Oscillator Strengths of CH-Stretching Transitions in Naphthalene Cation

	HF/I[a]	HF/I[b]	B3LYP/I[c]	B3LYP/II[c]
$\|1\rangle_\alpha$	4.03×10^{-6}	8.97×10^{-7}	2.58×10^{-7}	6.58×10^{-7}
$\|1\rangle_\beta$	8.14×10^{-8}	1.16×10^{-6}	4.15×10^{-7}	9.73×10^{-7}
$\|2\rangle_\alpha$	2.19×10^{-6}	2.90×10^{-6}	4.89×10^{-7}	3.37×10^{-7}
$\|2\rangle_\beta$	3.96×10^{-7}	1.40×10^{-6}	7.09×10^{-7}	4.68×10^{-7}
$\|3\rangle_\alpha$	2.02×10^{-7}	3.81×10^{-7}	6.42×10^{-8}	2.93×10^{-8}
$\|3\rangle_\beta$	2.29×10^{-7}	2.66×10^{-7}	9.45×10^{-8}	4.18×10^{-8}
$\|4\rangle_\alpha$	5.04×10^{-8}	1.41×10^{-7}	6.93×10^{-9}	3.02×10^{-9}
$\|4\rangle_\beta$	3.30×10^{-8}	2.70×10^{-8}	1.02×10^{-8}	4.28×10^{-9}
$\|5\rangle_\alpha$	5.88×10^{-9}	1.01×10^{-7}	9.26×10^{-10}	3.53×10^{-10}
$\|5\rangle_\beta$	1.92×10^{-9}	3.33×10^{-9}	1.26×10^{-9}	6.17×10^{-10}
$\|6\rangle_\alpha$	4.90×10^{-10}	4.34×10^{-8}	1.49×10^{-10}	4.78×10^{-11}
$\|6\rangle_\beta$	6.58×10^{-10}	1.89×10^{-9}	1.82×10^{-10}	1.09×10^{-10}

[a] D_{2h} structure. [b] C_{2h} structure with the intensities of nonequivalent CH_α (CH_β) oscillators added. [c] With Grid = 99434.

TABLE 7: Total Oscillator Strengths of the CH-Stretching Regions in Naphthalene

	calc				
v	HF/I	HF/II	B3LYP/I	B3LYP/II	exp[a]
1	3.51×10^{-5}	2.71×10^{-5}	3.08×10^{-5}	2.41×10^{-5}	1×10^{-5}
2	7.93×10^{-7}	6.86×10^{-7}	9.23×10^{-7}	6.99×10^{-7}	6×10^{-7}
3	1.55×10^{-7}	7.88×10^{-8}	1.84×10^{-7}	9.26×10^{-8}	9×10^{-8}
4	1.89×10^{-8}	7.75×10^{-9}	1.84×10^{-8}	7.96×10^{-9}	
5	2.48×10^{-9}	1.08×10^{-9}	2.23×10^{-9}	1.04×10^{-9}	

[a] Fundamental value from ref 30 and overtone values from ref 33.

in overtone intensities introduced with the 99434 integration grid is less than 10%. The uncertainty arising from the limitation to fifth order in the dipole moment expansion is also estimated to be about 10%.

Low lying electronic transitions have recently been observed for the naphthalene cation down to about 15000 cm^{-1}.[38] These electronic transitions should be significantly stronger than the overtones in the same region and the likelihood of observing the $\Delta v_{CH} \geq 6$ overtones is small.

We have compared intensity calculations for naphthalene cation with the HF/I, B3LYP/I and B3LYP/II methods. We have calculated intensities for both the C_{2h} and D_{2h} optimized structures with the HF/I method. Despite the similar geometries the two HF results are quite different as shown in Table 6. The relative intensities within a given overtone seem to fluctuate for successive overtones with no pattern, contrary to the B3LYP results and what is commonly observed.[10−13] In Table 6 we also compare B3LYP intensities calculated with the two basis sets. We see the usual decrease in intensity with increasing basis set size, apart from the fundamental region which shows approximately a factor of two increase in intensity. The fundamental intensity of the cation is of similar intensity to the first overtone. However, a one to two orders of magnitude decrease in intensity from the fundamental to first overtone is usually observed.[10−13]

The total calculated CH-stretching oscillator strengths in neutral naphthalene are given in Table 7. As expected, the present HF intensities are very close to our previous calculations at similar levels.[33] We see that the HF method leads to results which are similar to our B3LYP results. This is contrary to what we have found for the cationic species. We see the common trend that a larger basis sets leads to smaller intensities which are in better agreement with the experimentally observed intensities. The experimental fundamental intensity is from matrix isolation studies[30] and the intensities for the overtones are from long path length vapor phase conventional spectra.[33] The agreement between our B3LYP/II results and experiment is very good for the overtones.

The B3LYP/II calculated frequencies and band intensities for CH-stretching transitions in naphthalene and anthracene and their cations are given in Tables 8 and 9. The calculated frequencies of the CH-stretching overtone transitions increase from CH_α to CH_β (and CH_γ) in both neutral and cationic species. We see that all transitions in the cations are significantly blue shifted. The shifts increase from about 20 cm^{-1} at $\Delta v_{CH} = 1$ to 150−180 cm^{-1} at $\Delta v_{CH} = 6$. The frequencies of the transitions to the $|v\rangle_\alpha$ and $|v\rangle_\beta$ states in naphthalene are similar to those to the $|v\rangle_\beta$ and $|v\rangle_\gamma$ in anthracene, whereas the $|v\rangle_\alpha$ band in anthracene is at slightly lower frequency. This similarity is expected based on the calculated bond lengths.

The calculated relative intensities of the CH-stretching overtone transitions increase from CH_α to CH_β (and CH_γ) in both neutral and cationic species. The intensity of the transition to the $|v\rangle_\alpha$ state in naphthalene and to the $|v\rangle_\beta$ state in anthracene is very similar. However, the intensity of transitions to the $|v\rangle_\gamma$ state in anthracene is noticeably larger than the intensity to the $|v\rangle_\beta$ state in naphthalene.

The intensities of the transitions to the $|v\rangle_\beta$ and $|v\rangle_\gamma$ states in the anthracene cation are larger than those to the $|v\rangle_\alpha$ and $|v\rangle_\beta$ states in the naphthalene cation. The transitions to the $|v\rangle_\alpha$ state in anthracene and anthracene cation are the weakest transitions for each species. This might be expected based on the number of CH_α bonds compared to the number of each of the other bonds. However, the intensity of the CH_α band is less than half the intensity of the CH_β band. It is interesting that the intensity of the individual transitions within an overtone increase the

TABLE 8: Calculated Frequencies and Oscillator Strengths of CH-Stretching Transitions in Neutral and Cationic Naphthalene[a]

	naphthalene		naphthalene cation	
	$\tilde{\nu}$ (cm^{-1})	f	$\tilde{\nu}$ (cm^{-1})	f
$\|1\rangle_\alpha$	3036	1.06×10^{-5}	3062	6.58×10^{-7}
$\|1\rangle_\beta$	3053	1.35×10^{-5}	3076	9.73×10^{-7}
$\|2\rangle_\alpha$	5956	2.81×10^{-7}	6008	3.37×10^{-7}
$\|2\rangle_\beta$	5988	4.19×10^{-7}	6038	4.68×10^{-7}
$\|3\rangle_\alpha$	8759	3.63×10^{-8}	8840	2.93×10^{-8}
$\|3\rangle_\beta$	8806	5.62×10^{-8}	8884	4.18×10^{-8}
$\|4\rangle_\alpha$	11446	3.06×10^{-9}	11556	3.02×10^{-9}
$\|4\rangle_\beta$	11506	4.90×10^{-9}	11616	4.28×10^{-9}
$\|5\rangle_\alpha$	14016	4.05×10^{-10}	14157	3.53×10^{-10}
$\|5\rangle_\beta$	14089	6.37×10^{-10}	14233	6.17×10^{-10}
$\|6\rangle_\alpha$	16469	7.43×10^{-11}	16643	4.78×10^{-11}
$\|6\rangle_\beta$	16555	1.12×10^{-10}	16735	1.09×10^{-10}

[a] Calculated with B3LYP/II (99434 grid) dipole moment functions and local mode parameters from Table 2.

TABLE 9: Calculated Frequencies and Oscillator Strengths of CH-Stretching Transitions in Neutral and Cationic Anthracene[a]

	anthracene		anthracene cation	
	$\tilde{\nu}$ (cm^{-1})	f	$\tilde{\nu}$ (cm^{-1})	f
$\|1\rangle_\alpha$	3032	4.40×10^{-6}	3051	4.09×10^{-10}
$\|1\rangle_\beta$	3040	1.06×10^{-5}	3062	7.13×10^{-8}
$\|1\rangle_\gamma$	3050	1.60×10^{-5}	3073	1.91×10^{-8}
$\|2\rangle_\alpha$	5946	1.21×10^{-7}	5987	1.21×10^{-7}
$\|2\rangle_\beta$	5962	2.91×10^{-7}	6008	3.90×10^{-7}
$\|2\rangle_\gamma$	5984	5.24×10^{-7}	6031	6.27×10^{-7}
$\|3\rangle_\alpha$	8743	1.53×10^{-8}	8807	1.15×10^{-8}
$\|3\rangle_\beta$	8768	3.68×10^{-8}	8839	3.81×10^{-8}
$\|3\rangle_\gamma$	8800	6.94×10^{-8}	8874	6.22×10^{-8}
$\|4\rangle_\alpha$	11422	1.28×10^{-9}	11512	1.08×10^{-9}
$\|4\rangle_\beta$	11456	3.05×10^{-9}	11554	3.51×10^{-9}
$\|4\rangle_\gamma$	11500	6.03×10^{-9}	11602	5.89×10^{-9}
$\|5\rangle_\alpha$	13984	1.72×10^{-10}	14101	1.55×10^{-10}
$\|5\rangle_\beta$	14027	4.02×10^{-10}	14154	4.67×10^{-10}
$\|5\rangle_\gamma$	14083	7.71×10^{-10}	14215	8.04×10^{-10}
$\|6\rangle_\alpha$	16429	3.20×10^{-11}	16574	2.87×10^{-11}
$\|6\rangle_\beta$	16481	7.33×10^{-11}	16639	8.05×10^{-11}
$\|6\rangle_\gamma$	16549	1.33×10^{-10}	16713	1.39×10^{-10}

[a] Calculated with B3LYP/II (99434 grid) dipole moment functions and local mode parameters from Table 3.

further away the associated bond is from the center of the molecule. This can perhaps be understood by the following argument. The displacement of partial charge located further away from the center would have a larger effect on the overall dipole moment and lead to the larger intensity.

The simulated spectra of naphthalene, anthracene and their cations in the $\Delta v_{\mathrm{CH}} = 4$ region are shown in Figure 3. The spectra have been generated by convoluting the transitions in Tables 8 and 9 with Lorentzians with a fwhm of 60 cm^{-1}, a reasonable line width for room-temperature overtone spectra. The most suitable line width to use in the simulation of PAH spectra would depend on the experimental conditions.

The B3LYP/II calculated total CH-stretching intensities of the fundamental and overtone regions for the PAHs are given in Table 10. We observe the usual drop-off in total intensity with increasing v.[10−13] On a per CH bond basis, the total overtone intensity is approximately the same for naphthalene and anthracene but the distribution to individual transitions is significantly different, as seen in Tables 8 and 9. The total intensity decreases significantly from the neutral to cation for the fundamental region. However, for the overtones the total intensity is remarkably similar between the neutral and cationic species. The small calculated intensities of the fundamental CH-stretching transitions in the cations agrees with the lack of experimental observation.[30,31] The total intensities of the $\Delta v_{\mathrm{CH}} = 2$ region in the anthracene cation is an order of magnitude larger than the fundamental intensity. The significantly larger than expected overtone intensities for the cations should encourage new experimental efforts to observe them.

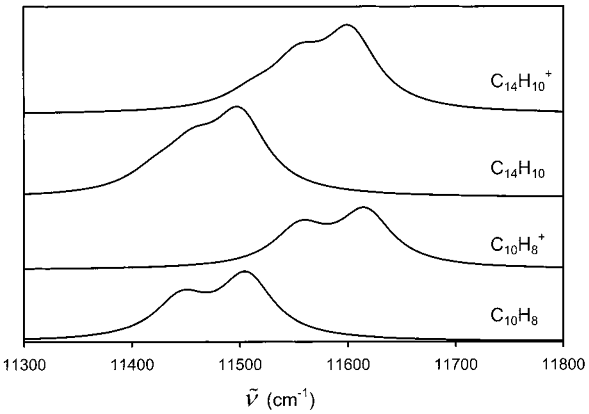

Figure 3. Simulated spectra of naphthalene and anthracene and their cations in the $\Delta v_{\mathrm{CH}} = 4$ region obtained with the B3LYP/II method. Each vibrational transition has been convoluted with a Lorentzian with a full width at half-maximum of 60 cm^{-1}.

TABLE 10: Calculated Total Oscillator Strengths of the CH-Stretching Bands in Neutral and Cationic Naphthalene and Anthracene[a]

v	$C_{10}H_8$	$C_{10}H_8^+$	$C_{14}H_{10}$	$C_{14}H_{10}^+$
1	2.41×10^{-5}	1.63×10^{-6}	3.10×10^{-5}	9.08×10^{-8}
2	6.92×10^{-7}	8.05×10^{-7}	9.36×10^{-7}	1.14×10^{-6}
3	9.25×10^{-8}	7.10×10^{-8}	1.22×10^{-7}	1.12×10^{-7}
4	7.96×10^{-9}	7.30×10^{-9}	1.04×10^{-8}	1.05×10^{-8}
5	1.04×10^{-9}	9.70×10^{-10}	1.35×10^{-9}	1.43×10^{-9}
6	1.86×10^{-10}	1.57×10^{-10}	2.38×10^{-10}	2.48×10^{-10}

[a] Calculated with B3LYP/II (99434 grid) dipole moment functions and local mode parameters from Tables 2 and 3.

Conclusion

We have calculated fundamental and overtone CH-stretching vibrational band frequencies and intensities of neutral and cationic naphthalene and anthracene. The calculations use a simple anharmonic oscillator local mode model and ab initio calculated dipole moment functions. We have used the previously determined experimental local mode frequencies and anharmonicities for naphthalene, and scaled ab initio calculated local mode parameters for anthracene and both cations, where overtone spectra have not yet been recorded. The ab initio calculations were performed at the HF and B3LYP levels of theory with the 6-31G(d) and 6-311+G(d,p) basis sets.

Our calculations show that the HF theory is not suitable for the calculation of fundamental and overtone spectra of cations, whereas the B3LYP method gives reasonable results. We find that the CH-stretching frequencies are blue shifted for the cations and that the intensities of the overtone transitions are similar in the neutral and cationic species. This is in stark contrast to the fundamental transitions which have significantly lower intensities for the cations than for the neutral molecules. This decrease in fundamental intensity for the cations is due to changes in the dipole moment function. Not surprisingly, CH-stretching fundamental intensities calculated with the double harmonic (DH) approximation differ from those calculated with the present anharmonic oscillator (AO) method by up to a factor of four for the cations. For the neutral molecules the discrepancy between the DH and AO intensities is about 20%.

Our calculations are in good agreement with the limited experimental data available. We believe that the B3LYP/6-311+G(d,p) calculated dipole moment functions and scaled local mode parameters in conjunction with the local mode method can provide an accurate estimate of CH-stretching overtone spectra of neutral and cationic polycyclic aromatic hydrocarbons. These simulated spectra could facilitate in determining the composition of the interstellar medium.

Acknowledgment. Funding for this research has been provided by the University of Otago. T.W.R. is grateful to the Foundation for Research, Science and Technology for a Bright Future Scholarship.

References and Notes

(1) Henry, B. R. *Acc. Chem. Res.* **1977**, *10*, 207.

(2) Mortensen, O. S.; Henry, B. R.; Mohammadi, M. A. *J. Chem. Phys.* **1981**, *75*, 4800.

(3) Child, M. S.; Lawton, R. T. *Faraday Discuss. Chem. Soc.* **1981**, *71*, 273.

(4) Sage, M. L.; Jortner, J. *Adv. Chem. Phys.* **1981**, *47*, 293.

(5) Henry, B. R. *Acc. Chem. Res.* **1987**, *20*, 429.

(6) Mortensen, O. S.; Ahmed, M. K.; Henry, B. R.; Tarr, A. W. *J. Chem. Phys.* **1985**, *82*, 3903.

(7) Findsen, L. A.; Fang. H. L.; Swofford, R. L.; Birge, R. R. *J. Chem. Phys.* **1986**, *84*, 16.

(8) Tarr, A. W.; Swanton, D. J.; Henry, B. R. *J. Chem. Phys.* **1986**, *85*, 3463.

(9) Tarr, A. W.; Zerbetto, F. *Chem. Phys. Lett.* **1989**, *154*, 273.

(10) Kjaergaard, H. G.; Yu, H.; Schattka, B. J.; Henry, B. R.; Tarr, A. W. *J. Chem. Phys.* **1990**, *93*, 6239.

(11) Kjaergaard, H. G.; Turnbull, D. M.; Henry, B. R. *J. Chem. Phys.* **1993**, *99*, 9438.

(12) Turnbull, D. M.; Kjaergaard, H. G.; Henry, B. R. *Chem. Phys.* **1995**, *195*, 129.

(13) Kjaergaard, H. G.; Proos, R. J.; Turnbull, D. M.; Henry, B. R. *J. Phys. Chem.* **1996**, *100*, 19273.

(14) Kjaergaard, H. G.; Henry, B. R. *Mol. Phys.* **1994**, *83*, 1099.

(15) Kjaergaard, H. G.; Daub, C. D.; Henry, B. R. *Mol. Phys.* **1997**, *90*, 201.

(16) Kjaergaard, H. G.; Bezar, K. J.; Brooking, K. A. *Mol. Phys.* **1999**, *96*, 1125.

(17) Kjaergaard, H. G.; Henry, B. R.; Wei, H.; Lefebvre, S.; Carrington, T., Jr.; Mortensen, O. S.; Sage, M. L. *J. Chem. Phys.* **1994**, *100*, 6228.

(18) Low, G. R.; Kjaergaard, H. G. *J. Chem. Phys.* **1999**, *110*, 9104.

(19) Vaida, V.; Daniel, J. S.; Kjaergaard, H. G.; Goss, L. M.; Tuck, A. F. Unpublished.

(20) Goss, L. M.; Sharpe, S. W.; Blake, T. A.; Vaida, V.; Brault, J. W. *J. Phys. Chem. A* **1999**, *103*, 8620.

(21) Daniel, J. S.; Solomon, S.; Sanders, R. W.; Portmann, R. W.; Miller, D. C.; Madsen, W. *J. Geophys. Res.* **1999**, *104*, 16785.

(22) Duley, W. W.; Williams, D. A. *Mon. Not. R. Astron. Soc.* **1981**, *196*, 269.

(23) Leger, A.; Puget, J. L. *Astron. Astrophys.* **1984**, *137*, L5.

(24) Allamandola, L. J.; Tielens, A. G. G. M.; Barker, J. R. *Astrophys. J.* **1985**, *290*, L25.

(25) Allamandola, L. J.; Tielens, A. G. G. M.; Barker, J. R. *Astr. J. Suppl. Ser.* **1989**, *71*, 733.

(26) Szczepanski, J.; Vala, M. *Nature* **1993**, *363*, 699.

(27) Fulara, J.; Lessen, D.; Freivogel, P.; Maier, J. P. *Nature* **1993**, *366*, 439.

(28) Snow, T. P.; Le Page, V.; Keheyan, Y.; Bierbaum, V. M. *Nature* **1998**, *391*, 259.

(29) Salama, F.; Allamandola, L. J. *Astrophys. J.* **1992**, *395*, 301.

(30) Szczepanski, J.; Vala, M. *Astrophys. J.* **1993**, *414*, 646.

(31) Hudgins, D. M.; Sandford, S. A.; Allamandola, L. J. *J. Phys. Chem.* **1994**, *98*, 4243.

(32) Ho, Y.-P.; Yang, Y.-C.; Klippenstein, S. J.; Dunbar, R. C. *J. Phys. Chem.* **1995**, *99*, 12115.

(33) Kjaergaard, H. G.; Henry, B. R. *J. Phys. Chem.* **1995**, *99*, 899.

(34) Kjaergaard, H. G.; Henry, B. R. *J. Phys. Chem.* **1996**, *100*, 4749.

(35) Langhoff, S. R. *J. Phys. Chem.* **1996**, *100*, 2819.

(36) Bauschlicher, C. W., Jr.; Langhoff, S. R. *Spectrochim. Acta* **1997**, *53*, 1225.

(37) Hudgins, D. M.; Sandford, S. A. *J. Phys. Chem. A* **1998**, *102*, 329, 344, 353.

(38) Romanini, D.; Biennier, L.; Salama, F.; Kachanov, A.; Allamandola, L. J.; Stoeckel, F. *Chem. Phys. Lett.* **1999**, *303*, 165.

(39) Atkins, P. W.; Friedman, R. S. *Molecular Quantum Mechanics*, 3rd ed.; Oxford University: Oxford, 1997.

(40) Sowa, M. G.; Henry, B. R.; Mizugai, Y. *J. Phys. Chem.* **1991**, *95*, 7659.

(41) Press, W. H.; Flannery, B. F.; Teukolsky, S. A.; Vetterling, W. T. *Numerical Recipes in C*; Cambridge University: Cambridge, 1988.

(42) Frisch, M. J.; Trucks, G. W.; Schlegel, H. B.; Gill, P. M. W.; Johnson, B. G.; Robb, M. A.; Cheeseman, J. R.; Keith, T. A.; Petersson, G. A.; Montgomery, J. A.; Raghavachari, K.; Al-Laham, M. A.; Zakrzewski, V. G.; Ortiz, J. V.; Foresman, J. B.; Cioslowski, J.; Stefanov, B. B.; Nanayakkara, A.; Challacombe, M.; Peng, C. Y.; Ayala, P. Y.; Chen, W.; Wong, M. W.; Andres, J. L.; Replogle, E. S.; Gomperts, R.; Martin, R. L.; Fox, D. J.; Binkley, J. S.; Defrees, D. J.; Baker, J.; Stewart, J. P.; Head-Gordon, M.; Gonzalez, C.; Pople, J. A. *Gaussian94*, Revision D.4; Gaussian, Inc.: Pittsburgh, PA, 1995.